



Design, microwave-mediated synthesis and biological evaluation of novel 4-aryl(alkyl)amino-3-nitroquinoline and 2,4-diaryl(dialkyl)amino-3-nitroquinolines as anticancer agents

Monika Chauhan^a, Anil Rana^a, Jimi Marin Alex^a, Arvind Negi^a, Sandeep Singh^b, Raj Kumar^{a,*,1}

^a Laboratory for Drug Design and Synthesis, Centre for Chemical and Pharmaceutical Sciences, School of Basic and Applied Sciences, Central University of Punjab, Bathinda 151 001, India

^b Centre for Genetic Diseases and Molecular Medicine, Central University of Punjab, Bathinda 151 001, India

ARTICLE INFO

Article history:

Received 28 August 2014

Available online 13 November 2014

Keywords:

Microwave heating
2,4-Diaminoquinolines
Synthesis
Anticancer activity
Molecular modeling

ABSTRACT

Design, microwave-assisted synthesis of novel 4-aryl (alkyl)amino-3-nitroquinoline (**1a–1l**) and 2,4-diaryl (dialkyl)amino-3-nitroquinolines (**2a–2k** and **3a**) via regioselective and complete nucleophilic substitution of 2,4-dichloro-3-nitroquinoline, respectively in water are presented. The newly synthesized compounds were evaluated for the first time for antiproliferative activity against EGFR overexpressing human lung (A-549 and H-460) and colon (HCT-116-wild type and HCT-116-p53 null) cancer cell lines. Some notions about structure–activity relationships (SAR) are presented. Compounds **2e**, **2f**, **2j** and **3a** overall exhibited excellent anticancer activity comparable to erlotinib which was used as a positive control. Molecular modeling studies disclosed the recognition pattern of the compounds and also supported the observed SAR.

© 2014 Elsevier Inc. All rights reserved.

1. Introduction

Immunomodulatory and antiproliferative imidazoquinolines [1,2] like imiquimod [3,4], and resiquimod [5] acting through activation of toll like receptors-7 (TLR-7) [6–9] and 3-nitroquinolines [10] as anticancer agents through epidermal growth factor receptor (EGFR) [11] inhibition are reported and are derived from a common precursor that is 4-amino(-2-halo)-3-nitroquinoline (Fig. 1). EGFR belongs to a receptor tyrosine kinase family and is found to be overexpressed in many of the cancers such as lung, colon, breast, etc. and is usually associated with poor prognosis [12]. EGFR is a validated druggable anticancer target and many inhibitors pertaining to several scaffolds like quinazolines, pyridopyrimidines, benzamides, indolinones and pyrrolotriazines targeting its ATP-binding domain have been reported [13]. Out of these, 4-anilinoquinazoline class is the most explored and represented the effective inhibition which is evident from the FDA approved drugs such as gefitinib, erlotinib and lapatinib [13].

In continuation to our interest in the synthesis of new chemical entities as anticancer agents [14–20], we thought of rationally

designing new EGFR inhibitors (**1–3**; Fig. 2) as anticancer agents through scaffold hopping [21] of previously reported quinazolines [13] and 3-nitroquinoline frameworks keeping in view that (a) substitution of C-2 hydrogen atom with a halogen may induce better interactions [13] due to the formation of a stable protein–ligand complex [22] and/or resistance to metabolism [23] or (b) an additional amino alkyl/aryl moiety at C-2 position may also enhance the EGFR inhibition due to the availability of extra space in the ATP binding pocket of EGFR [24] and, (c) the target compounds may also be able to bind with mutant type EGFR [25] (T790M [26,27] and L858R [28]) so that acquired resistance may not be the major problem of drug resistance as seen with the most of EGFR inhibitors.

For the synthesis of **1**, **2** and **3**, their precursor 2,4-dichloro-3-nitroquinoline (**4**) prepared [2] from commercially available 2,4-quinolinediol was thought to be substituted with diverse aryl/alkyl amines. The literature search carried out on aromatic nucleophilic substitution of haloquinolines such as 2,4-dihalo, 4,7-dihalo or 4-haloquinolines with aryl/alkyl amines highlighted their limited applications in generation of libraries of compounds and their scale-up as these methodologies suffer one or other disadvantages such as use of high boiling solvents like NMP [29] and DMF [30] that are difficult to remove, halogenated solvents like DCM [2] bases [2,29,30], acids [31,32], Pd catalysis [33] or other involving long reaction times (4–48 h) [29,31,32].

* Corresponding author.

E-mail addresses: raj.khunger@gmail.com, rajcps@cup.ac.in (R. Kumar).

¹ CUPB Library Communication Number: P109/14.

2. Materials and methods

2.1. Chemistry

All the reagents were of AR/GR quality and were purchased from Sigma–Aldrich, Loba-Chemie Pt. Ltd., S.D.F.C.L., Sisco Research Laboratory and HiMedia Laboratories Ltd. and were used without further purification. Sartorius analytical balance (BSA224S-CW) was used for the weighing purposes. Biotage Initiator microwave synthesizer was used for carrying out reaction. JSGW heating mantle, ILMVAC rotary evaporator was used for drying the compound. The progress of the reactions were monitored by TLC, using hexane/ethyl acetate and chloroform/methanol as the mobile phase on pre-coated Merck TLC plates in JSGW UV/fluorescent analysis cabinet and/or iodine chamber. Melting points were recorded on Stuart melting point apparatus (SMP-30) with open glass capillary tube and were uncorrected. IR spectra of compounds were recorded with KBr on a Bruker FT-IR spectrophotometer. NMR and HRMS experiments were performed at SAIF, Panjab University Chandigarh. ^1H NMR and ^{13}C NMR spectra were obtained in $\text{CDCl}_3/\text{d}_6\text{-DMSO}$ on 400 MHz and 100 MHz Bruker Avance II NMR spectrometer, respectively using TMS ($\delta = 0$) as an internal standard. All the target compounds were unreported (except **1a** and **1i**) and their physical data are presented as below.

2.1.1. 3-Nitroquinoline-2,4-diol (**4a**)

4a was synthesized using protocol reported in the literature. Mp 210–212 °C; IR (KBr, cm^{-1}): 3313 (OH stretch), 2850 (C–C stretch), 2350 (C=N stretch), 1522 (NO_2 stretch); ^1H NMR (CDCl_3 , 400 MHz, δ with TMS = 0): 12.00 (1H, s), 8.05–8.03 (1H, dd, $J_{12} = 1.2$ Hz; $J_{13} = 8.4$ Hz), 7.62–7.58 (1H, m), 7.35–7.33 (1H, d, $J = 8$ Hz), 7.26–7.22 (1H, m); ^{13}C NMR (CDCl_3 , 100 MHz, δ with TMS = 0): 157.11, 155.78, 138.21, 132.98, 126.41, 124.41, 122.06, 115.76, 113.77; MS (ESI): $m/z = 207.1$ [$\text{M} + 1$] $^+$.

2.1.2. 2,4-dichloro-3-nitroquinoline (**4b**)

4b was synthesized using protocol reported in the literature [2]. Mp 94–96 °C; IR (KBr, cm^{-1}): 1614 (C=N), 1490 (C=C), 1215 (C–N), 748 (C–Cl); ^1H NMR (CDCl_3 , 400 MHz, δ with TMS = 0): 8.28–8.26 (1H, dd, $J_{12} = 1.2$ Hz; $J_{13} = 8.8$ Hz), 8.13–8.10 (1H, d, $J = 8.4$ Hz), 7.97–7.92 (1H, m), 7.83–7.79 (1H, m); ^{13}C NMR (CDCl_3 , 100 MHz, δ with TMS = 0): 147.3, 144.78, 141.3, 132.19, 129.6, 128.6, 125.5, 124.4.

2.1.3. Synthesis of **1a–1j**: representative procedure for synthesis of *N*-benzyl-2-chloro-3-nitroquinolin-4-amine (**1a**)

To a reaction vial, a suspension of 2,4-dichloro-3-nitroquinoline (243 mg, 1 mmol) in water (1 mL) was added benzyl amine (0.11 mL, 1 equiv.) and the mixture was heated under microwave irradiation using Biotage initiator for 10 min at 80 °C. After the completion of the reaction (TLC), water was removed from mixture, dried and purified through column chromatography to afford **1a**.

2.1.4. *N*-benzyl-2-chloro-3-nitroquinolin-4-amine (**1a**)

Yield: 87%, Yellow solid [2], Mp 170–172 °C; IR (KBr, cm^{-1}): 3269 (NH stretch), 2278 (C=N stretch), 1512 (NO_2 stretch), 822 (C–Cl stretch); ^1H NMR (CDCl_3 , 400 MHz, δ with TMS = 0): 7.88 (1H, d, $J = 8$ Hz), 7.77 (1H, d, $J = 8.4$ Hz), 7.70–7.66 (1H, m), 7.45–7.41 (1H, m), 7.39–7.35 (3H, m), 7.32–7.30 (2H, m), 5.8 (D_2O exchangeable NH, s), 5.23 (s, 2H); HRMS (TOF-ESI) Calcd for $\text{C}_{16}\text{H}_{12}\text{ClN}_3\text{O}_2$, 313.0618 (M^+); observed: 314.0672 ($\text{M} + \text{H}$) $^+$.

All the remaining reactions were carried out using this general procedure with different substituted anilines.

2.1.5. 2-Chloro-*N*-(2-chlorobenzyl)-3-nitroquinolin-4-amine (**1b**)

Yield: 76%, Yellow solid, Mp 180–182 °C; ^1H NMR (CDCl_3 , 400 MHz, δ with TMS = 0): 8.44 (D_2O exchangeable NH, s), 8.10–8.06 (1H, m), 7.83 (1H, dd, $J_{12} = 0.8$ Hz, $J_{13} = 8$ Hz), 7.78–7.74 (1H, m), 7.61–7.50 (1H, m), 7.41–7.35 (2H, m), 7.31–7.24 (2H, m), 4.54 (2H, d, $J = 6$ Hz); ^{13}C NMR (CDCl_3 , 100 MHz, δ with TMS = 0): 145.4, 144.1, 141.2, 134.4, 132.4, 131.4, 129.0, 128.4, 126.6, 126.2, 122.7, 119.3, 45.0. HRMS (TOF-ESI) Calcd for $\text{C}_{16}\text{H}_{11}\text{Cl}_2\text{N}_3\text{O}_2$, 347.0228 (M^+); observed: 348.0230 ($\text{M} + \text{H}$) $^+$.

2.1.6. 2-Chloro-*N*-(4-fluorobenzyl)-3-nitroquinolin-4-amine (**1c**)

Yield: 78%, Yellow solid, Mp 150–152 °C; ^1H NMR (CDCl_3 , 400 MHz, δ with TMS = 0): 7.95 (1H, dd, $J_{12} = 0.8$ Hz; $J_{13} = 8.4$ Hz), 7.82 (1H, d, $J = 8.4$ Hz), 7.78–7.74 (1H, m), 7.54–7.50 (1H, m), 7.36–7.33 (2H, m), 7.14–7.09 (2H, m), 5.8 (D_2O exchangeable NH, s), 4.55 (2H, d, $J = 4.8$ Hz). HRMS (TOF-ESI) Calcd for $\text{C}_{16}\text{H}_{11}\text{ClFN}_3\text{O}_2$, 331.0524 (M^+); observed: 332.0620 ($\text{M} + \text{H}$) $^+$.

2.1.7. 2-Chloro-3-nitro-*N*-phenylquinolin-4-amine (**1d**)

Yield: 77%, Yellow solid, Mp 178–180 °C; IR (KBr, cm^{-1}): 3234 (NH stretch), 2212 (C=N stretch), 1568 (NO_2 stretch), 889 (C–Cl stretch); ^1H NMR (CDCl_3 , 400 MHz, δ with TMS = 0): 8.06 (D_2O exchangeable NH, s), 7.97 (1H, d, $J = 8.4$ Hz), 7.75–7.68 (2H, m), 7.34–7.30 (3H, m), 7.21–7.17 (1H, t, $J = 7.6$ Hz), 7.02 (2H, d,

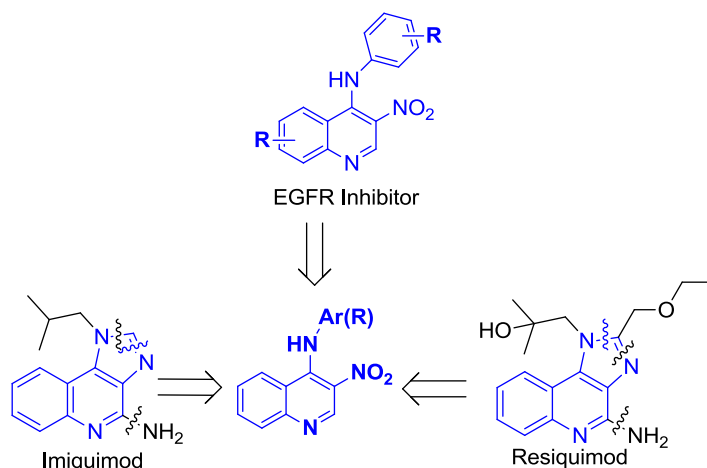


Fig. 1. Medicinal agents derived from 4-amino-3-nitroquinoline.

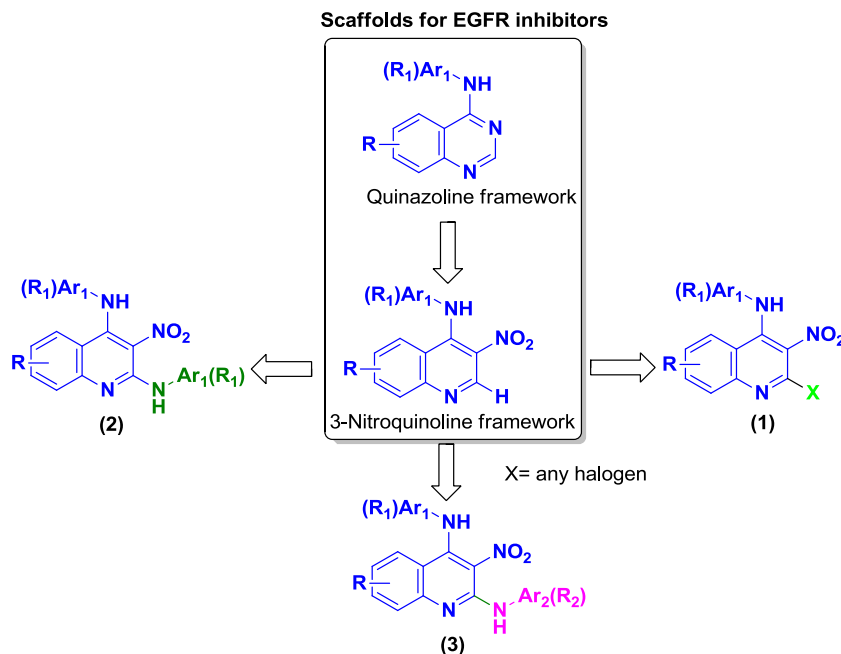


Fig. 2. Design of target compounds (1–3).

$J = 7.6$ Hz). HRMS (TOF-ESI) Calcd for $C_{15}H_{10}ClN_3O_2$, 299.0462 (M)⁺; observed: 300.0472 ($M + H$)⁺.

2.1.8. 2-Chloro-*N*-(2-methoxyphenyl)-3-nitroquinolin-4-amine (**1e**)

Yield: 73%, Yellow solid, Mp 230–232 °C; IR (KBr, cm^{-1}): 3259 (NH stretch), 2365 (C=N stretch), 1578 (NO_2 stretch), 854 (C–Cl stretch); 1H NMR ($CDCl_3$, 400 MHz, δ with TMS = 0): 8.03 (D_2O exchangeable NH, s), 7.96 (1H, d, $J = 8.4$ Hz), 7.90 (1H, d, $J = 8.52$ Hz), 7.78–7.73 (1H, m), 7.42–7.38 (1H, m), 7.17–7.12 (1H, m), 6.97 (1H, d, $J = 8.4$ Hz), 6.84 (2H, m), 3.87 (3H, s); HRMS (TOF-ESI) Calcd for $C_{16}H_{12}ClN_3O_3$, 329.0567 (M)⁺; observed: 330.0640 ($M + H$)⁺.

2.1.9. 2-Chloro-*N*-(4-methoxyphenyl)-3-nitroquinolin-4-amine (**1f**)

Yield: 81%, Yellow solid, Mp 142–144 °C; 1H NMR ($CDCl_3$, 400 MHz, δ with TMS = 0): 9.64 (D_2O exchangeable NH, s), 8.50 (1H, d, $J = 8.4$ Hz), 7.33–7.29 (3H, m), 7.08 (2H, d, $J = 8.8$ Hz), 6.83 (2H, d, $J = 8.8$ Hz), 3.8 (3H, s); ^{13}C NMR ($CDCl_3$, 100 MHz, δ with TMS = 0): 157.1, 145.8, 143.0, 141.3, 139.2, 131.7, 130.2, 128.8, 127.1, 126.3, 125.0, 123.7, 120.1, 113.6, 54.9. HRMS (TOF-ESI) Calcd for $C_{16}H_{12}ClN_3O_3$, 329.0567 (M)⁺; observed: 330.0570 ($M + H$)⁺.

2.1.10. 2-Chloro-*N*-(2-fluorophenyl)-3-nitroquinolin-4-amine (**1g**)

Yield: 77%, Yellow solid, Mp 170–172 °C; IR (KBr, cm^{-1}): 3252 (NH stretch), 2201 (C=N stretch), 1560 (NO_2 stretch), 762 (C–Cl stretch); 1H NMR ($CDCl_3$, 400 MHz, δ with TMS = 0): 8.01 (D_2O exchangeable NH, d, $J = 8$ Hz), 7.79–7.73 (3H, m), 7.42–7.37 (1H, m), 7.19–7.14 (2H, m), 7.05–7.01 (1H, m), 6.92 (1H, t, $J = 8.4$ Hz). HRMS (TOF-ESI) Calcd for $C_{15}H_9ClFN_3O_2$, 317.0367 (M)⁺; observed: 318.0468 ($M + H$)⁺.

2.1.11. 2-Chloro-*N*-(3-chloro-4-fluorophenyl)-3-nitroquinolin-4-amine (**1h**)

Yield: 72%, Yellow solid, Mp 188–190 °C; 1H NMR ($CDCl_3$, 400 MHz, δ with TMS = 0): 8.12 (1H, dd, $J_{12} = 2.4$ Hz; $J_{13} = 6.4$ Hz), 8.02 (1H, dd, $J_{12} = 1.2$ Hz; $J_{13} = 8.4$ Hz), 7.81–7.76 (1H, m), 7.70–7.63 (1H, m), 7.60–7.56 (1H, m), 7.44–7.38 (2H, m), 7.13 (1H, t, $J = 8.8$ Hz). HRMS (TOF-ESI) Calcd for $C_{15}H_8Cl_2FN_3O_2$, 351.9978 (M)⁺; observed: 352.1012 ($M + H$)⁺.

2.1.12. 2-Chloro-*N*-(4-methoxybenzyl)-3-nitroquinolin-4-amine (**1i**)

Yield: 91%, Yellow solid, Mp 210–212 °C [34]; 1H NMR ($CDCl_3$, 400 MHz, δ with TMS = 0): 7.92 (1H, dd, $J_{12} = 0.8$ Hz; $J_{13} = 8.4$ Hz), 7.82 (1H, dd, $J_{12} = 0.8$ Hz; $J_{13} = 8.8$ Hz), 7.76–7.72 (1H, m), 7.51–7.47 (1H, m), 7.29–7.26 (2H, m), 6.95–6.91 (2H, m), 5.87 (D_2O exchangeable NH, s), 4.47 (2H, d, $J = 4.8$ Hz), 3.81 (3H, s).

2.1.13. 2-Chloro-*N*-(3-methoxybenzyl)-3-nitroquinolin-4-amine (**1j**)

Yield: 88%, Yellow solid, Mp 162–164 °C; 1H NMR ($CDCl_3$, 400 MHz, δ with TMS = 0): 7.94 (1H, dd, $J_{12} = 1.2$ Hz; $J_{13} = 8.4$ Hz), 7.84 (1H, d, $J = 8.4$ Hz), 7.77–7.73 (1H, m), 7.53–7.48 (1H, m), 7.34 (1H, t, $J = 8$ Hz), 6.95–6.88 (3H, m), 5.98 (D_2O exchangeable NH, s), 4.54 (2H, d, $J = 4.8$ Hz), 3.87 (3H, s). HRMS (TOF-ESI) Calcd for $C_{17}H_{14}ClN_3O_3$, 343.0724 (M)⁺; observed: 344.0812 ($M + H$)⁺.

2.1.14. Synthesis of **2a–2k**: Representative procedure for synthesis of N^2,N^4 -dibenzyl-3-nitroquinoline 2,4-diamine (**2a**)

To a reaction vial, a suspension of 2,4-dichloro-3-nitroquinoline (243 mg, 1 mmol) in water (1 mL) was added benzyl amine (2 equiv) and the mixture was heated under microwave irradiation using Biotage initiator for 10 min at 120 °C. After the completion of the reaction (TLC), water was removed from mixture, dried and purified through column chromatography to afford **2a**.

2.1.15. N^2,N^4 -dibenzyl-3-nitroquinoline 2,4-diamine (**2a**)

Yield: 89%, Red solid, Mp 160–162 °C; IR (KBr, cm^{-1}): 3320 (NH stretch), 2256 (C=N stretch), 1489 (NO_2 stretch); 1H NMR ($CDCl_3$, 400 MHz, δ with TMS = 0): 10.4 (D_2O exchangeable NH, s), 8.6 (D_2O exchangeable NH, s), 7.83 (1H, d, $J = 8.8$ Hz), 7.46–7.43 (2H, m), 7.36–7.17 (10H, m), 6.96–6.92 (1H, m), 4.92 (2H, d, $J = 5.6$ Hz), 4.7 (2H, d, $J = 5.2$ Hz); ^{13}C NMR ($CDCl_3$, 100 MHz, δ with TMS = 0): 155.20, 150.65, 139.21, 137.15, 133.55, 129.28, 128.58, 128.00, 127.35, 126.69, 120.70, 118.27, 114.35, 53.94, 45.50; HRMS (TOF-ESI) Calcd for $C_{23}H_{20}N_4O_2$, 384.1586 (M)⁺; observed: 385.1135 ($M + H$)⁺.

All the remaining reactions were carried out using this general procedure with different substituted anilines.

2.1.16. *N*²,*N*⁴-bis(2-chlorobenzyl)-3-nitroquinoline-2,4-diamine (**2b**)

Yield: 81%, Red solid, Mp 165–167 °C; IR (KBr, cm⁻¹): 3250 (NH stretch), 2312 (C=N stretch), 1543 (NO₂ stretch), 792 (C–Cl stretch); ¹H NMR (CDCl₃, 400 MHz, δ with TMS = 0): 10.2 (D₂O exchangeable NH, s), 8.76 (D₂O exchangeable NH, s), 7.73 (1H, d, *J* = 8.4 Hz), 7.46 (3H, d, *J* = 4.8 Hz), 7.42–7.36 (2H, m), 7.32–7.30 (1H, m), 7.27–7.24 (2H, m), 7.16–7.12 (2H, m), 6.97–6.94 (1H, m), 4.98 (2H, d, *J* = 6 Hz), 4.88 (2H, d, *J* = 5.6 Hz); HRMS (TOF-ESI) Calcd for C₂₃H₁₈Cl₂N₄O₂, 452.0807 (M)⁺; observed: 453.0543 (M + H)⁺.

2.1.17. *N*²,*N*⁴-bis(4-fluorobenzyl)-3-nitroquinoline-2,4-diamine (**2c**)

Yield: 80%, Red solid, Mp 165–167 °C; ¹H NMR (CDCl₃, 400 MHz, δ with TMS = 0): 10.5 (D₂O exchangeable NH, s), 8.72 (D₂O exchangeable NH, s), 7.89 (1H, d, *J* = 8 Hz), 7.56–7.51 (2H, m), 7.42–7.38 (2H, m), 7.36–7.32 (2H, m), 7.12–6.99 (5H, m), 4.98 (2H, d, *J* = 5.6 Hz), 4.82 (2H, d, *J* = 5.2 Hz). HRMS (TOF-ESI) Calcd for C₂₃H₁₈F₂N₄O₂, 420.1398 (M)⁺; observed: 421.1401 (M + H)⁺.

2.1.18. 3-Nitro-*N*²,*N*⁴-diphenylquinoline-2,4-diamine (**2d**)

Yield: 75%, Red solid, Mp 152–154 °C; IR (KBr, cm⁻¹): 3212 (NH stretch), 2287 (C=N stretch), 1557 (NO₂ stretch), 807 (C–Cl stretch); ¹H NMR (CDCl₃, 400 MHz, δ with TMS = 0): 10.8 (D₂O exchangeable NH, s), 10.1 (D₂O exchangeable NH, s), 7.82 (2H, d, *J* = 8 Hz), 7.6 (1H, d, *J* = 8 Hz), 7.52–7.48 (2H, m), 7.41–7.32 (4H, m), 7.21 (1H, t, *J* = 7.2 Hz), 7.13 (3H, t, *J* = 7.6 Hz), 6.89–6.85 (1H, m); ¹³C NMR (CDCl₃, 100 MHz, δ with TMS = 0): 149.91, 147.28, 141.76, 139.11, 133.43, 129.71, 129.32, 128.83, 127.71, 125.82, 123.75, 122.85, 121.69, 115.43; HRMS (TOF-ESI) Calcd for C₂₁H₁₆N₄O₂, 356.1273 (M)⁺; observed: 357.1049 (M + H)⁺.

2.1.19. *N*²,*N*⁴-bis(2-methoxyphenyl)-3-nitroquinoline-2,4-diamine (**2e**)

Yield: 73%, Red solid, Mp 155–157 °C; IR (KBr, cm⁻¹): 3245 (NH stretch), 2245 (C=N stretch), 1556 (NO₂ stretch); ¹H NMR (CDCl₃, 400 MHz, δ with TMS = 0): 10.6 (D₂O exchangeable NH, s), 10.4 (D₂O exchangeable NH, s), 8.90–8.88 (1H, m), 7.71 (1H, dd, *J*₁₂ = 5.2 Hz; *J*₁₃ = 12.4 Hz), 7.59 (1H, d, *J* = 0.8 Hz), 7.57–7.50 (1H, m), 7.23 (1H, d, *J* = 14 Hz), 7.13–7.03 (2H, m), 6.96–6.83 (4H, m), 6.81–6.53 (1H, m), 3.97 (3H, s), 3.85 (3H, s). HRMS (TOF-ESI) Calcd for C₂₃H₂₀N₄O₄, 416.1485 (M)⁺; observed: 417.1521 (M + H)⁺.

2.1.20. *N*²,*N*⁴-bis(4-methoxyphenyl)-3-nitroquinoline-2,4-diamine (**2f**)

Yield: 85%, Red solid, Mp 95–97 °C; IR (KBr, cm⁻¹): 3265 (NH stretch), 2257 (C=N stretch), 1517 (NO₂ stretch); ¹H NMR (CDCl₃, 400 MHz, δ with TMS = 0): 11.27 (D₂O exchangeable NH, s), 10.22 (D₂O exchangeable NH, s), 7.71–7.68 (2H, m), 7.51 (1H, dd, *J*₁₂ = 1.6 Hz; *J*₁₃ = 9.2 Hz), 7.44 (2H, d, *J* = 1.2 Hz), 7.09 (2H, d, *J* = 8.8 Hz), 6.94 (2H, dd, *J*₁₂ = 2 Hz; *J*₁₃ = 6.8 Hz), 6.88 (2H, dd, *J*₁₂ = 2 Hz; *J*₁₃ = 7.2 Hz), 6.78 (1H, m), 3.84 (6H, s); HRMS (TOF-ESI) Calcd for C₂₃H₂₀N₄O₄, 416.1485 (M)⁺; observed: 417.1074 (M + H)⁺.

2.1.21. *N*²,*N*⁴-bis(2-fluorophenyl)-3-nitroquinoline-2,4-diamine (**2g**)

Yield: 79%, Red solid, Mp 120–122 °C; IR (KBr, cm⁻¹): 3278 (NH stretch), 2326 (C=N stretch), 1498 (NO₂ stretch); ¹H NMR (CDCl₃, 400 MHz, δ with TMS = 0): 10.4 (D₂O exchangeable NH, s), 10.3 (D₂O exchangeable NH, s), 8.12 (1H, d, *J* = 8.8 Hz), 7.97–7.93 (1H, m), 7.84–7.77 (2H, m), 7.21–7.09 (8H, m); HRMS (TOF-ESI) Calcd for C₂₁H₁₄F₂N₄O₂, 392.1085 (M)⁺; observed: 393.1010 (M + H)⁺.

2.1.22. *N*²,*N*⁴-bis(4-fluorophenyl)-3-nitroquinoline-2,4-diamine (**2h**)

Yield: 77%, Red solid, Mp 120–122 °C; IR (KBr, cm⁻¹): 3156 (NH stretch), 2387 (C=N stretch), 1534 (NO₂ stretch) 1237 (C–F stretch); ¹H NMR (CDCl₃, 400 MHz, δ with TMS = 0): 10.9 (D₂O

exchangeable NH, s), 10.1 (D₂O exchangeable NH, s), 7.72 (2H, q, *J* = 4 Hz), 7.58 (1H, d, *J* = 8.4 Hz), 7.51 (1H, m), 7.43 (1H, d, *J* = 8.8 Hz), 7.13–7.03 (6H, m), 6.89 (1H, m); ¹³C NMR (CDCl₃, 100 MHz, δ with TMS = 0): 161.73, 160.41, 159.28, 150.31, 149.34, 147.44, 137.80, 133.55, 127.83, 124.83, 123.62, 121.05, 115.54, 114.84; HRMS (TOF-ESI) Calcd for C₂₁H₁₄F₂N₄O₂, 392.1085 (M)⁺; observed: 393.0823 (M + H)⁺.

2.1.23. *N*²,*N*⁴-bis(3-ethynylphenyl)-3-nitroquinoline-2,4-diamine (**2i**)

Yield: 86%, Red solid, Mp 190–192 °C; ¹H NMR (CDCl₃, 400 MHz, δ with TMS = 0): 10.6 (D₂O exchangeable NH, s), 10.0 (D₂O exchangeable NH, s), 7.99 (1H, s), 7.79 (1H, d, *J* = 8.4 Hz), 7.64 (1H, d, *J* = 8 Hz), 7.54 (1H, t, *J* = 7.6 Hz), 7.47 (1H, d, *J* = 8.8 Hz), 7.35–7.24 (5H, m), 7.03 (1H, d, *J* = 8.4 Hz), 6.94 (1H, t, *J* = 7.6 Hz), 3.19 (1H, s), 3.10 (1H, s); ¹³C NMR (CDCl₃, 100 MHz, δ with TMS = 0): 149.2, 146.9, 141.9, 139.1, 133.6, 129.7, 129.3, 127.9, 127.4, 125.8, 125.0, 123.8, 123.0, 122.6, 122.1, 121.9, 115.2, 83.6, 82.4, 29.7. HRMS (TOF-ESI) Calcd for C₂₅H₁₆N₄O₂, 404.1273 (M)⁺; observed: 405.1375 (M + H)⁺.

2.1.24. *N*²,*N*⁴-bis(3-chloro-4-fluorophenyl)-3-nitroquinoline-2,4-diamine (**2j**)

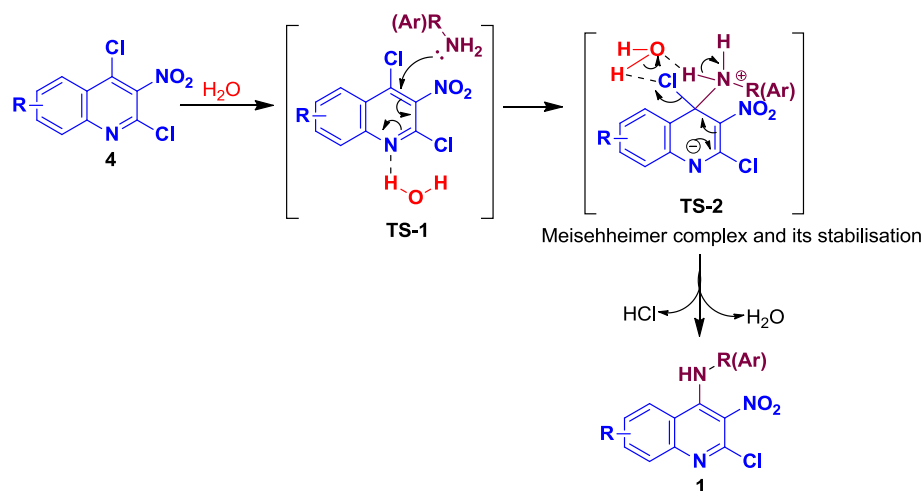
Yield: 83%, Red solid, Mp 168–170 °C; IR (KBr, cm⁻¹): 3421 (NH stretch), 2957 (C–C stretch), 1536 (NO₂ stretch), 773 (C–Cl stretch); ¹H NMR (CDCl₃, 400 MHz, δ with TMS = 0): 10.5 (D₂O exchangeable NH, s), 9.93 (D₂O exchangeable NH, s), 7.99 (1H, dd, *J*₁₂ = 2.8 Hz; *J*₁₃ = 6.8 Hz), 7.56–7.50 (2H, m), 7.48–7.43 (1H, m), 7.38 (1H, d, *J* = 8.4 Hz), 7.14 (1H, dd, *J*₁₂ = 2.8 Hz; *J*₁₃ = 6.4 Hz), 7.10 (2H, m), 6.92–6.86 (2H, m); HRMS (TOF-ESI) Calcd for C₂₁H₁₂Cl₂F₂N₄O₂, 460.0305 (M)⁺; observed: 461.0301 (M + H)⁺.

2.1.25. *N*²,*N*⁴-bis(3,4-dichlorophenyl)-3-nitroquinoline-2,4-diamine (**2k**)

Yield: 88%, 127 mg, Red solid, Mp: 154–156 °C; IR (KBr cm⁻¹): 3197 (NH stretch), 2287 (C=N stretch), 1546 (NO₂ stretch), 856 (C–Cl stretch); ¹H NMR (CDCl₃, 400 MHz) δ: 10.4 (D₂O exchangeable NH, s), 9.9 (D₂O exchangeable NH, s), 8.18 (1H, d, *J* = 2.4 Hz), 7.67 (1H, dd, *J*₁₂ = 0.8 Hz; *J*₁₃ = 8.4 Hz), 7.63–7.61 (1H, m), 7.57 (1H, dd, *J*₁₂ = 1.2 Hz; *J*₁₃ = 12 Hz), 7.50 (1H, dd, *J*₁₂ = 0.8 Hz; *J*₁₃ = 8.8 Hz), 7.42 (1H, d, *J* = 8.4 Hz), 7.37 (1H, d, *J* = 8.8 Hz), 7.22 (1H, d, *J* = 2.4 Hz), 7.06–7.02 (1H, m), 6.88 (1H, dd, *J*₁₂ = 2.8 Hz; *J*₁₃ = 8.8 Hz); ¹³C NMR (CDCl₃, 100 MHz) δ: 148.91, 148.61, 146.46, 141.30, 134.04, 131.25, 130.24, 128.16, 127.01, 126.65, 123.91, 123.29, 123.05, 121.50, 120.76, 115.31, 29.71; MS (ESI): HRMS (TOF-ESI) Calcd for C₂₁H₁₂Cl₄N₄O₂, 491.9714 (M)⁺; observed: 492.9812 (M + H)⁺.

2.1.26. Synthesis of *N*⁴-(2-chlorobenzyl)-*N*²-(4-methoxyphenyl)-3-nitroquinoline-2,4-diamine (**3a**)

To a reaction vial, a suspension of 2-chloro-*N*-(2-chlorobenzyl)-3-nitroquinolin-4-amine (347 mg, 1 mmol) in water (1 mL) was added *p*-anisidine (1equiv) and the mixture was heated under microwave irradiation using Biotage initiator for 25 min at 120 °C. After the completion of the reaction (TLC), water was removed from mixture, dried and purified through column chromatography to afford **3a**. Yield: 84%, Red solid, Mp 201–203 °C; ¹H NMR (CDCl₃, 400 MHz, δ with TMS = 0): 10.9 (D₂O exchangeable NH, s), 10.1 (D₂O exchangeable NH, s), 7.88 (1H, d, *J* = 8.4 Hz), 7.63–7.59 (2H, m), 7.50–7.43 (2H, m), 7.34–7.30 (2H, m), 7.13 (1H, t, *J* = 7.6 Hz), 7.08–7.01 (2H, m), 6.93–6.91 (1H, m), 6.85–6.82 (1H, m). HRMS (TOF-ESI) Calcd for C₂₃H₁₉ClN₄O₃, 434.1146 (M)⁺; observed: 435.1204 (M + H)⁺.



Scheme 1. Plausible mechanism for the regioselective S_NAr in water under MW heating.

2.2. Biology

2.2.1. Cell culture and treatments

All the cell lines were procured from National cell repository situated at NCCS, Pune. lung (A-549 and H-460), colon (HCT-116-wild type and HCT-116-p53 null) and EGFR low expressing breast fibroadenoma (MCF-7) [35,36] cancer cell lines representing different human cancers were grown in DMEM media supplemented with 10% fetal bovine serum (FBS) and antibiotic solution (1× Pen-strip, all the reagents from Invitrogen). Buccal cavity cells were harvested and culture according to the earlier described protocol by Weisberg et al. [37,38]. Briefly the mouth was rinsed at least 2 h before with mouthwash. Cells were harvested in PBS and washed three times with antibiotic containing PBS to remove the contaminants. Cells were cultured in DMEM media with 10% FBS, 50 U/ml penicillin G, 50 µg/ml streptomycin sulfate and 1.25 µg/ml amphotericin B (fungizone). The cells were incubated at 37 °C

with 5% CO₂ and 95% humidity conditions. For experiments, cells were seeded in equal numbers after trypan blue cell counting (5000 cells per well of 96-well plate and 100,000 cells per well of 6 well plate). Afterwards cells were washed once with sterile 1× PBS and cultured with serum free media for 8 h for synchronization. The test compounds were dissolved in cell culture grade DMSO up to concentration of 100 mM and further dilutions were done in serum free DMEM media. The total amount of media per well (200 µL per well of 96 well plate and 2 mL per well for six well plates) was kept constant and all the treatment volumes were accommodated within these ranges only.

2.2.2. 3-(4,5-Dimethylthiazol-2-yl)-2,5-diphenyl tetrazolium bromide (MTT) assay

MTT assay was carried out in 96-well plates where total volume of media was 200 µl/well. Briefly cells after the treatments were washed with 1× PBS and were mixed with 100 µl/ml well of

Table 1

Optimization of the reaction conditions for the syntheses of *N*-benzyl-2-chloro-3-nitroquinolin-4-amine (**1a**) and *N*²,*N*⁴-dibenzyl-3-nitroquinoline-2,4-diamine (**2a**)

Entry	Solvent	Equiv (amine)	Temp (°C)	Time (h)	Yield ^a (1a:2a) ^{b,c}
1	Neat	1	80	1	10 ^d (58:42)
2	Neat	2	120	1	15 ^d (36:64)
3	DMF ^e	1	80	1.5	85 (60:40)
4	DMF ^e	2	120	1.5	89 (20:80)
5	NMP ^e	1	80	1.5	82 (58:42)
6	NMP ^e	2	120	1.5	84 (15:85)
7	MeOH ^e	1	80	20 min	85 (80:20)
8	MeOH ^e	2	120	20 min	87 (21:79)
9	H ₂ O ^e	1	80	10 min	87 (100:0)
10	H ₂ O ^e	2	120	10 min	89 (0:100)
11	Toluene ^e	1	80	3	71 (43:57)
12	Toluene ^e	2	120	3	72 (35:65)

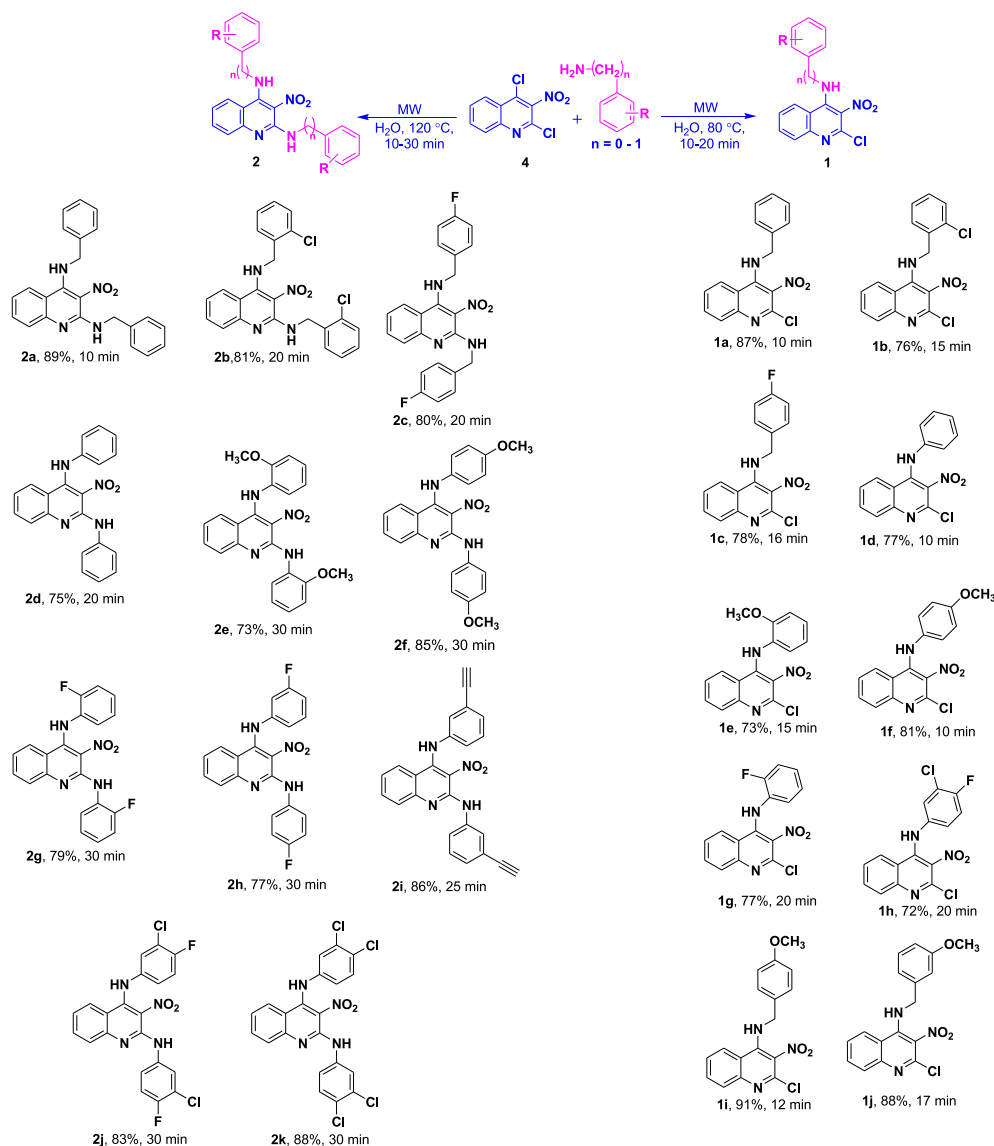
^a A stirred mixture of **4** (1 mmol) and benzylamine (1 equiv or 2 equiv) in a sealed vial was heated under microwave irradiations using Biotage Initiator.

^b Isolated yield.

^c Ratio obtained after column chromatographic purification.

^d Trace amount of products were obtained in carrying out the reaction under conventional heating at 100 °C for 12 h.

^e 1 mL of solvent was used.



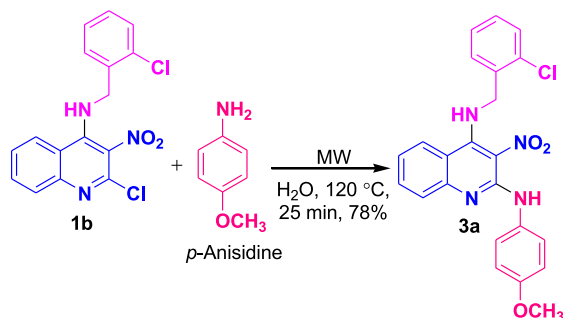
Scheme 2. Synthesis of target compounds (1a–1i and 2a–2k).

MTT (5 mg in 10 ml of $1 \times$ PBS) and incubated at room temperature in dark for 4 h to allow formation of formazan crystals. Each well was then mixed with 100 μ l of DMSO to dissolve the crystals followed by ELISA readings at 570 nm. The percent growth inhibition was calculated by the following formula: $(1 - [A_{570\text{treated}}/A_{570\text{control}}]) \times 100\%$. Then IC_{50} values were calculated from the above data. The results were then represented as obtained after averaging three independent experiments.

2.3. Molecular modeling

3-Dimensional co-crystal structure of EGFRwt with erlotinib was retrieved from Protein Data Bank (PDB 1M17) and was further edited for protein preparation by removing excess crystallized water molecules (using Accelrys discovery studio visualizer 3.5), adding of polar hydrogens and charges (using Autodock [39]). This protonation step also corrects the ionization and tautomeric states of amino acid residues and therefore modifies the total Gasteiger charges on the protein structure, which were calculated as -2.0061 . Chemical structures of ligands were drawn in Chem3D-Pro and minimized by MM2 force-field where 1000 iteration cycles were run, to get the steepest energy minimized structure. The Grid

was generated with the aid of AutoGrid MGL tools 1.5.6rc3 module of Autodock, which is a user defined 3-dimensional grid particular selecting the atoms of the kinase domain for docking. In the present study, the location and dimensions of the grid box was taken from the coordinates ($x:y:z::4.66:-0.23:-5.507$) of the centroid of the already embedded molecule (erlotinib), with the help of Accelrys discovery studio visualizer 3.5 [40]. This domain involves major portion of ATP active binding site, where this site is enzymatic active region of the EGFR. The energy scoring grid was prepared as $60 \times 60 \times 60$ (x,y,z) cube. The spacing between grid points was 0.375 Å. This larger size was taken as to rationalize the ligand binding mode over the selected amino acid residues. Each docking experiment was done by implicating the Lamarckian Genetic Algorithm (LGA) [41] which was set with the total 1000 conformations, 50 different runs with termination after 250,000 energy evaluation. Population size was set out to be 150. Finally, the conformation of lowest predicted binding free energy of the most occurring binding modes in the EGFR active pocket was selected. To validate the adopted docking procedure, the co-crystallized structure of erlotinib was extracted from the PDB 1M17 and further docked at the ATP binding site of EGFR. The RMSD value of 0.967 Å between co-crystallized and docked conformation



Scheme 3. Synthesis of N^4 -(2-chlorobenzyl)- N^2 -(4-methoxyphenyl)-3-nitroquinoline-2,4-diamine.

of erlotinib validates and warrants the reliability of the adopted docking procedure.

3. Results and discussion

3.1. Optimization of the reactions conditions for the synthesis of 4-aryl(alkyl) amino-3-nitroquinoline and 2,4-diaryl(dialkyl) amino-3-nitroquinolines

Now a days, microwave (MW) assisted reactions producing drug and drug intermediates are becoming popular due to the rapid generation of libraries of compounds in lesser time, high yields, efficient and rapid dielectric heating of the reaction mixture in a sealed vessel to temperatures even above the boiling point of the solvent [42–44]. In order to determine the optimum reaction conditions for regioselective (C-4 or C-2-substituted product) as well as complete nucleophilic substitution of **4**, a model reaction of **4** (1 mmol) with benzylamine (1 or 2 equiv) was carried out under MW heating under different reaction conditions; the results are shown in Table 1. There was practically no product formation under neat conditions (TLC). Although the isolated yields of the product(s) (**1a** and or **2a**) were more than 80% under almost all the polar solvents but we could not get the regioselective formation of **1a** i.e. C-4 substituted product or complete S_NAr leading to **2a** (except in water and to some extent in methanol) in spite of the fact that C-4 position of quinoline (if an electron withdrawing group is at C-3) is more reactive for nucleophilic substitution than C-2 [45,46]. The highest product distribution with respect to the formation of products **1a** and **2a** was obtained in carrying out the reactions under water at 80 and 120 °C, respectively for 10 min (entries **9** and **10**). Both the compounds (**1a** and **2a**) formed were removed from the water, dried and purified through column chromatography.

The regioselective C-4 (**1a**) substituted product formation in protic polar solvents like methanol and water under MW irradiations could probably be due to the reason [47] that these solvents increase the reactivity at C-4(Cl) position as they may assist in electron delocalization toward the nitrogen atom of quinoline through H-bond formation (TS-1, Scheme 1). In addition to it, water could stabilize the corresponding Meisenheimer complex [48] via “ambiphilic dual activation” [43,49] by polar interactions with the halogen (C-4) of quinoline and the hydrogen atom of the positively charged amine (TS-2). Whereas this kind of stabilization is less likely to happen with C-2 (Cl) because of α -aza effect [47] in which the corresponding Meisenheimer complex might not get greatly influenced by the hydroxylic solvents probably due to the internal neutralization of the negative charge through an intramolecular hydrogen bonding of the amine hydrogen to the aza group [47].

3.2. Synthesis of 4-aryl(alkyl) amino-3-nitroquinoline and 2,4-diaryl(dialkyl) amino-3-nitroquinolines

To prove the generality of the reaction and synthesize a variety of mono and diaminoquinoline compounds, **4** was treated with diverse aryl/arylalkyl amines under the optimized conditions using microwave in water for 10–30 min. The reactions were found to be compatible with aliphatic and aromatic amines with a variety of substitution. All the compounds (**1a–1l** and **2a–2k**; Scheme 2) formed were removed from the water, dried and purified (72–91%) through column chromatography and well characterized.

The regioselective C-4 substituted product formation of the compounds (**1a–1l**) was confirmed chemically when **1f** upon acid hydrolysis with a mixture of acetic acid and water for 8 h yielded the corresponding quinilin-2-one. The IR spectrum of this compound showed a characteristic absorption of $-\text{CONH}-$ at 1647 cm^{-1} which was indicative of formation of quinilin-2-one but not quinilin-4-one which absorb below 1600 cm^{-1} .

For the synthesis of target compounds **3**, **1a** was heated in water with *p*-anisidine (1 equiv) for 25 min under microwave irradiations that successfully afforded **3a** (Scheme 3; 78%). This further extended the scope of the present methodology for the synthesis of diaminoquinolines having differently substituted aryl/alkyl amines at positions-2 and 4.

All the target compounds were unreported (except **1a** and **1i**) and fully characterized by mp, NMR, IR and HRMS techniques.

3.3. Antiproliferative activity

We selected the EGFR overexpressing human lung (A-549 [50] and H-460) and colon (HCT-116-wild type [51] and HCT-116-p53 null) cell lines for the screening of the final compounds (**1a–1l**, **2a–2k** and **3a**). Erlotinib was used as the positive control [52]. Among the series of twenty-two compounds, four compounds **2e**, **2f**, **2j** and **3a** overall inhibited the growth of lung and colon cancer cell lines with IC_{50} ranging from $4.8\text{ }\mu\text{M}$ to $11.2\text{ }\mu\text{M}$ (Table 2). Compounds **2f** and **2j** were found to possess significant antiproliferative activity against both lung cancer cell lines with $\text{IC}_{50\text{s}}$ (μM) = 5.4 (H-460), 6.5 (A-549) and 7.1 (H-460), 11.2 (A-549), respectively comparable to erlotinib. Interestingly, **2e** and **3a** selectivity and significantly inhibited the growth of colon carcinoma (HCT-116-p53 null) with $\text{IC}_{50\text{s}}$ (μM) = 5.1 and 4.8, respectively whereas other compounds also showed equal or better efficiency, indicating that their mode of action is p53 independent. p53 is reported to be mutant in almost half of the total cancers [53] where many of the existing anticancer drugs fail. The result of current study shows that such compounds may lead to better effect against p53 mutant cancers. Selected compounds (**2e**, **2f**, **2j** and **3a**) were further evaluated and showed no significant cytotoxicity toward human buccal cavity cells at the highest concentration of $100\text{ }\mu\text{M}$. This overall endorses that the compounds are cytotoxic selectively to cancer cells owing to the reason that these compounds upon metabolism get accumulated in the cancer cell [54]. In order to establish the EGFR specificity of the compounds; **2e**, **2j** and **3a** were screened against EGFR low expression breast fibroadenoma cancer cell line (MCF-7) [35,36] for their anti-proliferative properties. The IC_{50} values obtained by MTT assay for **2e**, **2j** and **3a** were found to be 42, >100 and $45\text{ }\mu\text{M}$, respectively. Our results show that due to low expression of EGFR in these cells, IC_{50} values for all the compounds were very high compared to other cancer cell lines. The overall results indicate that these compounds are unable to exhibit anti-proliferative activity in MCF-7 cell line due to low EGFR expression suggestive of their EGFR dependent growth inhibition.

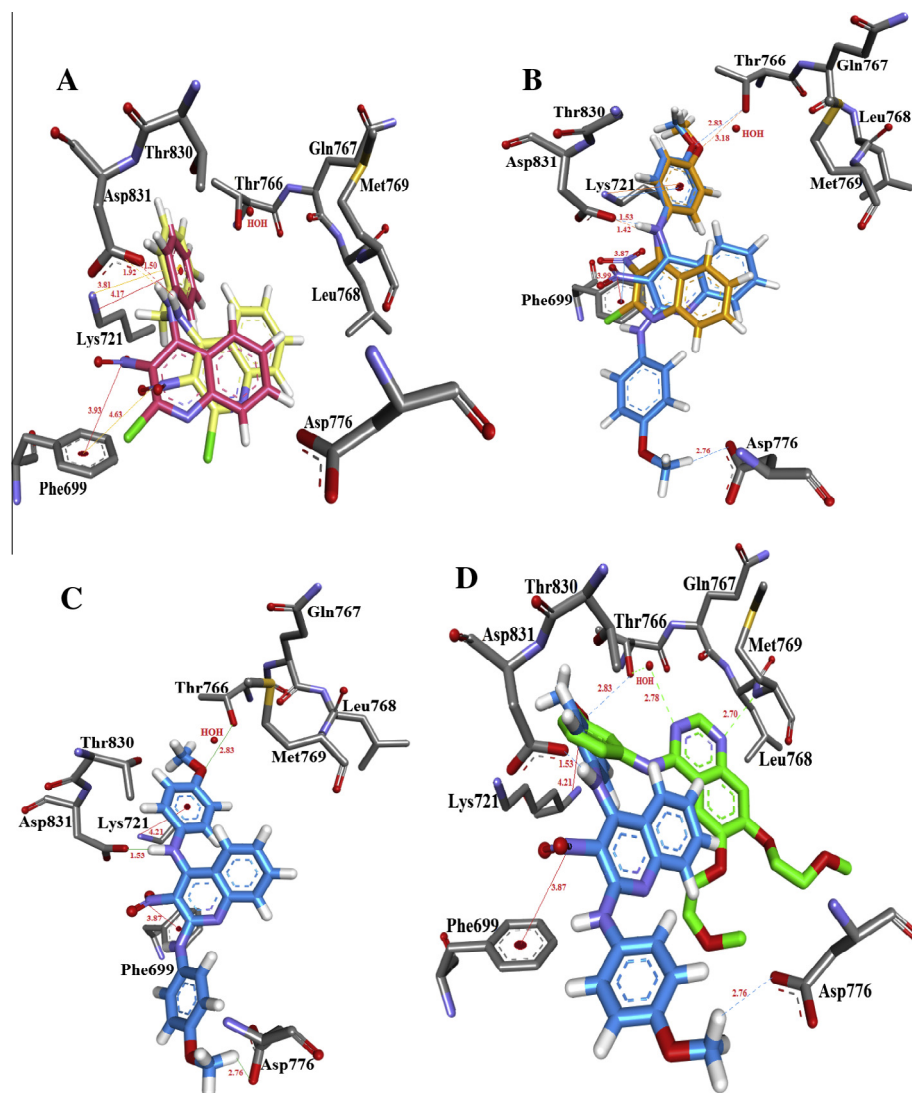


Fig. 3. Various binding poses (perspective views) of compounds inside the EGFR kinase ATP binding site: (A) binding interactions of **1a** (yellow) and **1d** (red) with kinase domain of EGFR. (B) Binding interactions of the **1f** (orange) and **2f** (blue). (C) Binding interactions of **2f** (orange). (D) Superposition of **2f** (blue) and erlotinib (green) poses in the kinase domain.

3.4. Structure–activity relationships

Some general trends about structure–activity relationships noticed from these studies on the target compounds (Table 2) are as follows: (a) change of substituted or unsubstituted dibenzylamines with substituted or unsubstituted dianilines at position –2 and/or –4 of 3-nitroquinoline resulted in immense increase in the cytotoxic activity (**2a** < **2d** and **1a** < **1d**) (b) substituents like electron donating or withdrawing groups at aniline ring of **2d** irrespective of the position favored the increase in activity (**2d** < **2e–2k**) whereas this trend was not observed when group(s) were kept on the aniline ring of **1d** (c) 2,4-dianilino/2,4-dibenzylaminoquinolines (**2d–2k/2a–2c**) exhibited higher anticancer activity as compared to 4-anilino/4-benzylaminoquinolines (**1d–1h/1a–1c** and **1i–1j**) except **3a** which selectively inhibited the growth of colon carcinoma HCT-116-p53 null type, and (d) quinoline with 4-fluoro-3-chloroaniline group (**2j**) was more cytotoxic as compared to 3,4-dichloroaniline (**2k**).

3.5. Molecular modeling

In order to theoretically investigate the binding mode of novel aminoquinazolines with the active site of EGFRwt (wild type;

PDB 1M17 [56]; complexed with erlotinib) based on the data obtained from the EGFR overexpressing cell growth inhibitory activity and molecular reasons to support the observed structure–activity relationships, molecular dockings of selected compounds **1a**, **1d**, **1f** and **2f** into the ATP-binding domain of EGFR were performed using Autodock software [39]. According to the results obtained with flexible docking of all the evaluated compounds occupying the erlotinib binding pocket, some common interactions with the residual amino acids of kinase domain were observed (Fig. 3) which are as follows: (i) π -cation interactions of **Phe699** with nitrogen atom of $-\text{NO}_2$ group and ϵ -amino group of **Lys721** with the 4-aryl substituent on the quinoline ring and (ii) hydrogen bond (H -bond) acceptor interaction of **Asp831** with $-\text{NH}$ functionality of 4-amino aryl substituent. The observed decrease in the anticancer activity (**1a**) upon incorporation of a methylene group in **1d** could be explained by the weaker π -cation interactions of **Phe699** (4.63 Å) and H -bond acceptor interaction of **Asp831** (1.92 Å) in **1a** as compared to **1d** (3.93 Å and 1.50 Å, respectively; Fig. 3A). The slight improvement in activity (**1f**) after incorporation of $p\text{-OCH}_3$ at 4-anilino ring in **1d** could be due to its additional H -bond acceptor interaction with **Thr766** (Fig. 3B). Further, the enhanced anticancer activity observed with **2f** might be due to the additional interaction of **2f** in comparison to **1f** where

Table 2Anticancer activity of the target compounds (**1a–1l**, **2a–2k** and **3a**).

Cd	A-549 (lung cancer)	H-460 (lung cancer)	HCT-116-wild type (colon carcinoma)	HCT-116-p53 null (colon carcinoma)
	<i>IC₅₀ values (μM)^a</i>			
1a	58.2	60.1	52.8	67.4
1b	56.1	51.3	49.7	69.1
1c	53.8	48.2	51.1	64.4
1d	38.2	42.9	43.1	52.1
1e	36.8	38.7	40.1	>70
1f	37.2	45.3	36.3	48.7
1g	32.9	42.7	33.3	34.6
1h	34.1	39.5	39.1	48.9
1i	53.4	59.2	49.7	>70
1j	57.2	51.1	54.3	>70
2a	40.2	43.1	50.6	>70
2b	45.2	41.7	43.9	69.3
2c	46.6	44.1	42.3	66.2
2d	19.2	25.5	26.3	61.0
2e	16.1	21.7	15.3	5.1
2f	6.5	5.4	20.1	19.8
2g	18.3	20.2	17.3	>70
2h	22.3	29.6	20.2	>70
2i	15.2	17.4	20.6	46.1
2j	11.2	7.1	24.1	52.3
2k	14.8	18.3	27.0	32.3
3a	>70	15.8	>70	4.8
Erlotinib ^b	12 [52]	8.30 [52]	7 [55]	– ^c

^a Values are derived from averaging three independent experiments and each experiment was done in triplicate.^b Used as positive control.^c Not tested.

its *p*-OCH₃C₆H₄NH group at 2-position of quinoline ring gets positioned near **Asp776** and interacts through *H*-bond donation (2.76 Å, Fig. 3C and D). Some of the known EGFR inhibitors e.g. erlotinib, gefitinib and lapatinib interact with some crucial amino acids of ATP kinase domain such as **Met769** (amide H-bond interaction with N-1 of erlotinib [56])/ **Met793** (amide H-bond interaction with N-1 of gefitinib [57] and lapatinib [58]), **Thr766** (interactions with N-3 of erlotinib [56] via H-bond bridge formation through H₂O molecule), **Lys745**, **Leu788**, and **Thr790** (surrounds aniline ring of gefitinib [57]). Overall all the tested molecules occupied the same EGFR binding pocket but with somewhat newer and different interactions with amino acid residues as compared to co-crystallised erlotinib and other reported inhibitors.

4. Conclusions

We have designed and developed easy and straightforward microwave-assisted synthesis of 4-aryl (alkyl)amino-3-nitroquinoline and 2,4-diaryl (dialkyl)amino-3-nitroquinolines *via* regioselective and complete S_NAr of 2,4-dichloro-3-nitroquinoline, respectively. The optimization of the synthetic procedure was carried out and the effect of various solvents under microwave irradiations on S_NAr was studied. Water emerged as the best suitable medium for carrying out the S_NAr. Following the optimized procedure, twenty-two target compounds were synthesized out of which twenty were found as novel. Most of the compounds exhibited significant anticancer activity against lung and colon cancer cell lines. Compounds **2e**, **2f**, **2j** and **3a** presented potent anticancer activity at low micromolar concentrations comparable to erlotinib. Cell survival assay in colon cancer cells indicated that the compounds exert their antiproliferative action independent of p53. Further studies on the molecular interventions on inhibition of signal transduction by **2f**, **2j** and **3a** are under progress and will be published in due course.

Acknowledgments

RK and MC thank DST, New Delhi for the financial assistance (F.No. SR/FT/CS-71/2011). Support from Research Seed Money

(RSM) from CUPB is also acknowledged. Authors also thank Prof. Tapas Mukhopadhyay for providing HCT-116-p53 null colon cancer cell line.

Appendix A. Supplementary material

Supplementary data associated with this article can be found, in the online version, at <http://dx.doi.org/10.1016/j.bioorg.2014.11.004>.

References

- [1] C.E. Schiaffo, C. Shi, Z. Xiong, M. Olin, J.R. Ohlfest, C.C. Aldrich, D.M. Ferguson, J. Med. Chem. 57 (2) (2014) 339–347.
- [2] N.M. Shukla, S.S. Malladi, C.A. Mutz, R. Balakrishna, S.A. David, J. Med. Chem. 53 (11) (2010) 4450–4465.
- [3] M. Stanley, Clin. Exp. Dermatol. 27 (7) (2002) 571–577.
- [4] S. Bozrova, V. Levitsky, S. Nedospasov, M. Drutskaya, Biochem. (Moscow) Suppl. Series B: Biomed. Chem. 7 (2) (2013) 136–145.
- [5] T. Meyer, C. Surber, L.E. French, E. Stockfleth, Exp. Opin. Invest. Drugs 22 (1) (2013) 149–159.
- [6] E. Vacchelli, L. Galluzzi, A. Eggermont, W.H. Fridman, J. Galon, C. Sautès-Fridman, E. Tartour, L. Zitvogel, G. Kroemer, Oncoimmunology 1 (6) (2012) 894.
- [7] L. Galluzzi, E. Vacchelli, A. Eggermont, W.H. Fridman, J. Galon, C. Sautès-Fridman, E. Tartour, L. Zitvogel, G. Kroemer, Oncoimmunology 1 (5) (2012) 699–716.
- [8] E. Vacchelli, A. Eggermont, C. Sautès-Fridman, J. Galon, L. Zitvogel, G. Kroemer, L. Galluzzi, Oncoimmunology 2 (8) (2013). e25238–e25238-14.
- [9] D. Spaner, Y. Shi, D. White, J. Mena, C. Hammond, J. Tomic, L. He, M. Tomai, R. Miller, J. Booth, Leukemia 20 (2) (2006) 286–295.
- [10] H.-H. Li, H. Huang, X.-H. Zhang, X.-M. Luo, L.-P. Lin, H.-L. Jiang, J. Ding, K.-X. Chen, H. Liu, Acta Pharmacol. Sin. 29 (12) (2008) 1529–1538.
- [11] R.S. Herbst, Int. J. Radiat. Oncol. Biol. Phys. 59 (2) (2004) S21–S26.
- [12] N. Normanno, A. De Luca, C. Bianco, L. Strizzi, M. Mancino, M.R. Maiello, A. Carotenuto, G. De Feo, F. Caponigro, D.S. Salomon, Gene 366 (1) (2006) 2–16.
- [13] M.L.d.C. Barbosa, L.M. Lima, R. Tesch, C.M.R. Sant'Anna, F. Totzke, M.H. Kubbutat, C. Schächtele, S.A. Laufer, E.J. Barreiro, Eur. J. Med. Chem. 71 (2014) 1–14.
- [14] A.T. Baviskar, U.C. Banerjee, M. Gupta, R. Singh, S. Kumar, M.K. Gupta, S. Kumar, S.K. Raut, M. Khullar, S. Singh, Bioorg. Med. Chem. 21 (18) (2013) 5782–5793.
- [15] S. Kumar, S. Sapra, R. Kumar, M.K. Gupta, S. Koul, T. Kour, A.K. Saxena, O.P. Suri, K.L. Dhar, Med. Chem. Res. 21 (11) (2012) 3720–3729.
- [16] S.S. Malhi, A. Budhiraja, S. Arora, K.R. Chaudhari, K. Nepali, R. Kumar, H. Sohi, R.S. Murthy, Int. J. Pharm. 432 (1) (2012) 63–74.
- [17] A. Negi, P. Ramarao, R. Kumar, Mini Rev. Med. Chem. 13 (5) (2013) 653–681.

- [18] A. Rana, J.M. Alex, M. Chauhan, G. Joshi, R. Kumar, *Med. Chem. Res.* (2014), <http://dx.doi.org/10.1007/s00044-014-1196-5>.
- [19] J.M. Alex, S. Singh, R. Kumar, *Arch. Pharm.* 347 (2014) 1–11.
- [20] G. Kaur, R.P. Cholia, A.K. Mantha, R. Kumar, J. Med. Chem. (2014), <http://dx.doi.org/10.1021/jm500865u>.
- [21] H. Mauser, W. Guba, *Curr. Opin. Drug Discov.* 11 (3) (2008) 365–374.
- [22] M.Z. Hernandes, S.M.T. Cavalcanti, D.R.M. Moreira, J. de Azevedo, W. Filgueira, A.C.L. Leite, *Curr. Drug Targets* 11 (3) (2010) 303–314.
- [23] R. Wilcken, M.O. Zimmermann, A. Lange, A.C. Joerger, F.M. Boeckler, *J. Med. Chem.* 56 (4) (2013) 1363–1388.
- [24] M.E. Noble, J.A. Endicott, L.N. Johnson, *Science* 303 (5665) (2004) 1800–1805.
- [25] W. Zhou, D. Ercan, L. Chen, C.-H. Yun, D. Li, M. Capelletti, A.B. Cortot, L. Chirieac, R.E. Jacob, R. Padera, *Nature* 462 (7276) (2009) 1070–1074.
- [26] W. Pao, V.A. Miller, K.A. Politi, G.J. Riely, R. Somwar, M.F. Zakowski, M.G. Kris, H. Varmus, *PLoS Med.* 2 (3) (2005) e73.
- [27] C.-H. Yun, K.E. Mengwasser, A.V. Toms, M.S. Woo, H. Greulich, K.-K. Wong, M. Meyerson, M.J. Eck, *Proc. Natl. Acad. Sci. USA* 105 (6) (2008) 2070–2075.
- [28] J.G. Paez, P.A. Janne, J.C. Lee, S. Tracy, H. Greulich, S. Gabriel, P. Herman, F.J. Kaye, N. Lindeman, T.J. Boggon, *Science* 304 (5676) (2004) 1497–1500.
- [29] I. Chiyanzu, C. Clarkson, P.J. Smith, J. Lehman, J. Gut, P.J. Rosenthal, K. Chibale, *Bioorg. Med. Chem.* 13 (9) (2005) 3249–3261.
- [30] T. Izumi, J. Sakaguchi, M. Takeshita, H. Tawara, K.-I. Kato, H. Dose, T. Tsujino, Y. Watanabe, H. Kato, *Bioorg. Med. Chem.* 11 (12) (2003) 2541–2550.
- [31] M. Ferlin, B. Gatto, G. Chiarello, M. Palumbo, *Bioorg. Med. Chem.* 8 (6) (2000) 1415–1422.
- [32] L. He, H.-X. Chang, T.-C. Chou, N. Savaraj, C. Cheng, *Eur. J. Med. Chem.* 38 (1) (2003) 101–107.
- [33] C. Wolf, R. Lerebours, *J. Org. Chem.* 68 (18) (2003) 7077–7084.
- [34] T.A. Kshirsagar, P.D. Heppner, S.E. Langer, Preparation of aminoimidazoquinolins as inducers of IFN- α biosynthesis for treatment of viral and neoplastic disease, WO2007056112A2, 2007.
- [35] C. Mamot, D.C. Drummond, U. Greiser, K. Hong, D.B. Kirpotin, J.D. Marks, J.W. Park, *Cancer Res.* 63 (12) (2003) 3154–3161.
- [36] J. Kao, K. Salari, M. Bocanegra, Y.-L. Choi, L. Girard, J. Gandhi, K.A. Kwei, T. Hernandez-Boussard, P. Wang, A.F. Gazdar, *PLoS One* 4 (7) (2009) e6146.
- [37] J.H. Weisburg, D.B. Weissman, T. Sedaghat, H. Babich, *Basic Clin. Pharmacol. Toxicol.* 95 (4) (2004) 191–200.
- [38] H. Babich, M. Krupka, H.A. Nissim, H.L. Zuckerbraun, *Toxicol. In Vitro* 19 (2) (2005) 231–242.
- [39] G.M. Morris, R. Huey, A.J. Olson, *Curr. Protoc. Bioinform.* (2008) 8–14.
- [40] D.S. Visualizer, Accelrys Software Inc., San Diego, CA, USA 2012.
- [41] G.M. Morris, D.S. Goodsell, R.S. Halliday, R. Huey, W.E. Hart, R.K. Belew, A.J. Olson, *J. Comp. Chem.* 19 (14) (1998) 1639–1662.
- [42] (a) C.O. Kappe, *Chem. Soc. Rev.* 37 (6) (2008) 1127–1139; (b) C.O. Kappe, B. Pieber, D. Dallinger, *Angew. Chem. Int. Ed.* 52 (4) (2013) 1088–1094.
- [43] D. Kumar, R. Kumar, *Tet. Lett.* 55 (16) (2014) 2679–2683.
- [44] H.F. Motiwala, R. Kumar, A.K. Chakraborti, *Aust. J. Chem.* 60 (5) (2007) 369–374.
- [45] W. Steinschifter, W. Stadlbauer, *J. Prakt. Chem.* 336 (4) (1994) 311–318.
- [46] R. Mekheimer, *J. Chem. Soc., Perkin Trans. 1* (15) (1999) 2183–2188.
- [47] G. Illuminati, G. Marino, G. Sleiter, *J. Am. Chem. Soc.* 89 (14) (1967) 3510–3515.
- [48] M. Schlosser, T. Rausis, *Helv. Chim. Acta* 88 (6) (2005) 1240–1249.
- [49] G.L. Khatik, R. Kumar, A.K. Chakraborti, *Org. Lett.* 8 (11) (2006) 2433–2436.
- [50] R. Diaz, P.A. Nguewa, R. Parrondo, C. Perez-Stable, I. Manrique, M. Redrado, R. Catena, M. Collantes, I. Penuelas, J.A. Diaz-Gonzalez, *BMC Cancer* 10 (1) (2010) 188.
- [51] T. Matsuo, S.S. Nishizuka, K. Ishida, T. Iwaya, M. Ikeda, G. Wakabayashi, *BMC Res. Notes* 4 (1) (2011) 140.
- [52] Y.-H. Ling, M. Aracil, J. Jimeno, R. Perez-Soler, Y. Zou, *Eur. J. Cancer* 45 (10) (2009) 1855–1864.
- [53] T. Soussi, K.G. Wiman, *Cancer Cell.* 12 (4) (2007) 303–312.
- [54] A. Rajapakse, C. Linder, R.D. Morrison, U. Sarkar, N.D. Leigh, C.L. Barnes, J.S. Daniels, K.S. Gates, *Chem. Res. Toxicol.* 26 (4) (2013) 555–563.
- [55] F. Morgillo, E. Martinelli, T. Troiani, M. Oditura, F. De Vita, F. Ciardiello, *PLoS One* 6 (12) (2011) e28841.
- [56] J. Stamos, M.X. Sliwkowski, C. Eigenbrot, *J. Biol. Chem.* 277 (48) (2002) 46265–46272.
- [57] C.-H. Yun, T.J. Boggon, Y. Li, M.S. Woo, H. Greulich, M. Meyerson, M.J. Eck, *Cancer Cell.* 11 (3) (2007) 217–227.
- [58] A.G. Evdokimov, M. Pokross, R. Walter, M. Mekel, B. Cox, C. Li, R. Bechard, F. Genbauffe, R. Andrews, C. Diven, *Acta Crystallogr. D. Biol. Crystallogr.* 62 (12) (2006) 1435–1445.